

Silencing rapsyn *in vivo* decreases acetylcholine receptors and augments sodium channels and secondary postsynaptic membrane folding

Pilar Martínez-Martínez^{a,*}, Marko Phernambucq^a, Laura Steinbusch^a, Laurent Schaeffer^b,
Sonia Berrih-Aknin^c, Hans Duimel^d, Peter Frederik^d, Peter Molenaar^a, Marc H. De Baets^{a,e}, Mario Losen^a

^a Department of Neuroscience, School of Mental Health and Neuroscience, Maastricht University, Maastricht, The Netherlands, PO Box 616, 6200 MD Maastricht, The Netherlands

^b Équipe Différenciation Neuromusculaire, Institut Fédératif de Recherche 128, Unité Mixte de Recherche 5161, Centre National de la Recherche Scientifique; École Normale Supérieure de Lyon, 46 allée d'Italie, 69364 Lyon Cedex 07, France

^c CNRS-UMR 8162, IPSC, Université Paris XI, Hôpital Marie Lannelongue, France

^d Electron Microscopy Unit, Department of Pathology, Maastricht University, Maastricht, The Netherlands

^e Neuroimmunology Group, Biomedical Research Institute (BIOMED) Hasselt University, Diepenbeek, Belgium

ARTICLE INFO

Article history:

Received 30 November 2008

Revised 23 February 2009

Accepted 18 March 2009

Available online 1 April 2009

Keywords:

Rapsyn

Voltage gated sodium channel

Myasthenia gravis

Neuromuscular junction

Congenital myasthenic syndromes

ABSTRACT

The receptor-associated protein of the synapse (rapsyn) is required for anchoring and stabilizing the nicotinic acetylcholine receptor (AChR) in the postsynaptic membrane of the neuromuscular junction (NMJ) during development. Here we studied the role of rapsyn in the maintenance of the adult NMJ by reducing rapsyn expression levels with short hairpin RNA (shRNA). Silencing rapsyn led to the average reduction of the protein levels of rapsyn (31% loss) and AChR (36% loss) at the NMJ within 2 weeks, corresponding to previously reported half life of these proteins. On the other hand, the sodium channel protein expression was augmented (66%) in rapsyn-silenced muscles. Unexpectedly, at the ultrastructural level a significant increase in the amount of secondary folds of the postsynaptic membrane in silenced muscles was observed. The neuromuscular transmission in rapsyn-silenced muscles was mildly impaired. The results suggest that the adult NMJ can rapidly produce postsynaptic folds to compensate for AChR and rapsyn loss.

© 2009 Elsevier Inc. All rights reserved.

Introduction

The postsynaptic apparatus of the skeletal neuromuscular junction (NMJ) is specialized to respond continuously and accurately to the neurotransmitter acetylcholine (ACh) released from the overlying nerve terminal. The acetylcholine receptor (AChR) is clustered at high density in the postsynaptic membrane by the receptor-associated protein of the synapse (rapsyn). Rapsyn is required for the organization of the developing NMJ since rapsyn-deficient mice lack differentiated NMJs and die shortly after birth (Gautam et al., 1995). In these mice, both presynaptic and postsynaptic abnormalities were found, including the lack of AChR clusters, lack of postsynaptic membrane folding, excessive nerve sprouting and decreased nerve terminal arborization.

Abbreviations: α -BT, α -bungarotoxin; AChR, acetylcholine receptor; CMAP, compound muscle action potential; CMS, congenital myasthenic syndrome; EMG, electromyography; EAMG, experimental autoimmune myasthenia gravis; MAC, membrane attack complex; mAb, monoclonal antibody; MG, myasthenia gravis; NMJ, neuromuscular junction; shRNA, short hairpin RNA; VAcHT, vesicular acetylcholine transporter; VGSC, voltage gated sodium channel.

* Corresponding author. Fax: +31 43 3671096.

E-mail address: p.martinez@np.unimaas.nl (P. Martínez-Martínez).

Available online on ScienceDirect (www.sciencedirect.com).

Mutations in the promoter or the coding sequence of the human *RAPSN* gene can cause congenital myasthenic syndromes (CMS). Decreased recruitment of AChR to rapsyn clusters, as well as decreased rapsyn expression at the endplate is likely to account for the endplate AChR deficiency (Cossins et al., 2006; Engel and Sine, 2005; Hantai et al., 2004; Maselli et al., 2003a; Ohno et al., 2002) resulting in an impaired neuromuscular transmission. In patients with the N88K rapsyn mutation (either homozygous or heteroallelic with other missense or promoter mutations) simplified postsynaptic membranes with few folds were found (Ohno et al., 2002, 2003).

The AChR clustering by rapsyn is strongly enhanced by nerve agrin (Brockhausen et al., 2008; Nitkin et al., 1987), which acts via Irf4, the receptor for agrin, and the muscle specific tyrosine kinase (MuSK) (DeChiara et al., 1996; Kim et al., 2008; Zhang et al., 2008). Agrin increases the half life of the AChR from 1 day to 10 days in muscle fibers (Bezakova et al., 2001). This process is entirely dependent on rapsyn, since silencing rapsyn *in vivo* completely prevents agrin-induced AChR clustering (Kong et al., 2004). Agrin deficient mice show very similar pre- and postsynaptic structural abnormalities as rapsyn-deficient mice (Gautam et al., 1996). In MMP3 null mice, which have increased synaptic levels of agrin, increased postsynaptic membrane folding has been observed (VanSaun et al., 2003). These observations suggest the possibility that agrin enhances both pre- and postsynaptic specialization via rapsyn. In line with this idea, β -

catenin, which interacts directly with rapsyn (Zhang et al., 2007), is required for retrograde signaling from the muscle to the nerve to ensure normal nerve branching in the muscle, normal localization of nerve terminals in narrow endplate bands and efficient acetylcholine release (Li et al., 2008).

Because rapsyn is crucial for the stabilization of the AChR it might also play a role in the autoimmune disease myasthenia gravis (MG) where auto-antibodies against the AChR reduce the number of functional AChRs at the postsynaptic membrane (Toyka et al., 1975). In rats and mice, expression of rapsyn increases with age (Brockhausen et al., 2008; Gervasio et al., 2007; Hoedemaekers et al., 1998) and thereby stabilizes the AChR (Gervasio and Phillips, 2005). In a passive transfer rat model for MG, increased expression of rapsyn at the NMJ induces resistance against anti-AChR antibodies (De Baets et al., 2003; Losen et al., 2005) by reducing antibody-induced AChR internalization. Conversely, rapsyn upregulation has a detrimental effect in chronic experimental autoimmune myasthenia gravis (EAMG) where endplates are already substantially damaged. In chronic EAMG, increased rapsyn expression increases postsynaptic membrane turnover by anti-AChR antibodies (Martínez-Martínez et al., 2007).

In order to obtain further insight into the role of rapsyn in adult muscle, we studied the effect of down-regulation of rapsyn by RNA interference (RNAi). Previous studies using long double strand RNA based RNAi *in vivo* had shown that rapsyn is essential for induction of ectopic AChR clusters following injection of neuronal agrin in extrasynaptic muscle areas (Kong et al., 2004). Here, we used RNAi to study the effect of rapsyn on the already matured endplates. Adult muscles of rats were transfected by *in vivo* electroporation using the mammalian expression vector pSUPER that directs the synthesis of short hairpin RNA (shRNA) transcripts. The results suggest that rapsyn has a pivotal role for the postsynaptic folding and the maintenance of the AChR in the NMJ of adult muscle.

Methods

Silencing constructs

Four DNA sequences for transcription of siRNA were selected according to Tuschl rules (Elbashir et al., 2001; Tuschl et al., 1999) from the coding DNA sequences of rapsyn conserved between rat (XM_215773) and mouse (J03962) (Table 1). The designed DNA oligonucleotides contained 19 nt sequences from rapsyn separated by a short spacer from the reverse complement of the same sequence. The corresponding pairs of DNA oligos were annealed and ligated into pSUPER digested with BglIII and HindIII as previously described (Brummelkamp et al., 2002) and all constructs were sequenced. The efficiency of the different rapsyn silencing pSUPER was measured *in vitro* by co-transfecting the silencing pSuper constructs with a (mouse-) rapsyn-GFP expression vector (Marchand et al., 2002) and the pSV- β -galactosidase expression vector (Promega, USA) in HEK 293 cells. The pSUPER empty vector was used as a negative control. HEK cells were cultured in DMEM with 10% heat-inactivated fetal bovine serum and transfected using the Profection Mammalian Transfection system with calcium phosphate (Promega). Cells were fixed in 4% paraformaldehyde in PBS at different time points after

transfection (24, 48 and 72 h). The transfection efficiency was measured by β -galactosidase enzyme assay of cell extracts; the proportion of transfected cells was analyzed by *in situ* staining of the cells for β -galactosidase activity using X-gal. Fluorescence images of rapsyn-GFP were obtained with an Olympus IX-71 inverted microscope before fixation of cells. X-gal staining of fixed and cover slipped cells was photographed using an Olympus AX-70 microscope. Pictures were analyzed using the ImageJ software (version 1.32; <http://rsb.info.nih.gov/ij>).

Animals

6-week-old female Lewis rats were obtained from the Department of Experimental Animal Services, Maastricht University, The Netherlands, with permission from the Committee on Animal Welfare, according to Dutch governmental rules. For immunization, *in vivo* electroporation and electromyography measurements, the animals were anesthetized with 3% isoflurane in air, supplied over a cylindrical cap held over the head. The animals were euthanized by CO₂/air inhalation and subsequent cervical dislocation.

Triple electroporation

The different DNAs were prepared for electroporation with the Qiagen Maxiprep kit, according to the manufacturer's manual, and finally dissolved at a concentration of 2 μ g/ μ L in 0.9% NaCl. The injection mix contained: 25 μ g of each silencing vector S-1, S-2, S-3 and S-4 and 50 μ g of pVax- β -galactosidase (Promega) in a total volume of 75 μ L. For the contralateral muscle, 100 μ g empty pSUPER and 50 μ g of pVax- β -galactosidase in a volume of 75 μ L were used. The electroporation in the tibialis anterior was performed with the same parameters as described previously (Losen et al., 2005) using the Electro Square Porator ECM 830 (BTX, San Diego, USA, for setup see Supplementary Fig. S1). This electroporation was repeated three times each other day under the same conditions.

Induction of EAMG

14 days after the first electroporation the rats were divided into two groups: half of the animals received no further treatment (control animals) the other half received intraperitoneal injections of the anti-AChR antibody mAb 35 (20 pmol per 100 g body weight; EAMG animals). After another 2 days, the rats were clinically scored, anesthetized for electromyography and sacrificed. Clinical scoring was performed by blinded investigators as previously described (Hoedemaekers et al., 1997a,b; Verschuuren et al., 1990).

Alpha-bungarotoxin treatment

α -BT (Sigma, USA) was injected into the tibialis anterior muscle directly at a dose of 2–5 μ g for 15 days, with injections every 48 h. Sham-treated animals were injected with saline at the same time points. Each day, to check for a possible imminent, accumulating overdose of α -BT, the rats were clinically scored on a scale of + to +++ on the basis of the drooping of the lower lip and salivation;

Table 1

Primer sequences for silencing rapsyn using pSUPER.

S-1 f:	5'-GATCCCCTGAGAAGCTATGTGAGTTTtcaagagaAAACTCACATAGCTTCTCATTTTTGGAAA-3'
S-1 r:	5'-AGCTTTTCCAAAATGAGAAGCTATGTGAGTTTtctctttaaAAACTCACATAGCTTCTCAGGG-3'
S-2 f:	5'-GATCCCCGGACTATGAGAAGCCCTGttcaagagaCAGGGCTTCTCATAGTCTTTTTGGAAA-3'
S-2 r:	5'-AGCTTTTCCAAAAGGACTATGAGAAGCCCTGtctctttaaCAGGGCTTCTCATAGTCCGGG-3'
S-3 f:	5'-GATCCCCGGCTTTGGATGCCATTGAGttcaagagaCTCAATGGCATCCAAGCCTTTTTGGAAA-3'
S-3 r:	5'-AGCTTTTCCAAAAGCCTTTGGATGCCATTGAGtctctttaaCTCAATGGCATCCAAGCCGGG-3'
S-4 f:	5'-GATCCCCGTGAGCCAGCTCAAGCTGttcaagagaCAGCTTGAGCTGGCTCAGCTTTTTGGAAA-3'
S-4 r:	5'-AGCTTTTCCAAAAGCTGAGCCAGCTCAAGCTGtctctttaaCAGCTTGAGCTGGCTCAGCCGG-3'

depending on the outcome of the score the next dose of α -BT was assessed to obtain a clinical effect of + or ++. Using this treatment regimen, blocked AChRs are replaced at a rate of about 10% per day so that the degree of AChR block ranged from about 95–100% (on the day of α -BT injection) down to about 80% 48 h later (just before the next α -BT injection) (Molenaar et al., 1991).

Electromyography (EMG)

Decrement of compound muscle action potential (CMAP) was measured simultaneously in both tibialis anterior muscles of 8 control and 9 EAMG rats. Stimulation of the peroneal nerve at the level of the knee and recording of the tibialis anterior muscles was performed as described before (Losen et al., 2005). To detect a decrement in the response, series of 8 supramaximal stimuli were given at 3 Hz with 0.2 ms stimulus duration. The test was considered positive for decrement when both the amplitude and the area of the negative peak of the CMAP showed a decrease of at least 10% (Kimura, 2001). To demonstrate reproducibility, at least 3 recordings were made of all investigated muscles. During the measurements, skin temperature was kept between 35 °C and 37 °C by means of a heating pad. If no decrement was observed initially, repeated small doses of curare (tubocurarine chloride, Sigma, 0.5 μ g in EAMG animals; between 1.5 μ g up to 6 μ g in control animals) were injected intraperitoneally with intervals of 10 min until the test was positive. Up to 3 μ g of curare in EAMG animals and up to 16.5 μ g of curare in control animals were used (c.f. Janssen et al., 2008; Seybold et al., 1976). The simultaneous recording of the CMAP during repetitive stimulation of both tibialis anterior muscles was used for measuring the lowest curare dose to produce a reproducible decremental response in each leg.

Histochemical staining

Isolated tibialis anterior muscles of several animals were frozen in melting isopentane. Cryosections of 10 μ m were stained for beta-galactosidase activity. The sections were warmed to 40–60 °C for 3 min, air dried for 1 h, fixed in 2.0% glutaraldehyde in PBS for 20 min at room temperature, washed 3 \times in PBS for 5 min and dried. Sections were then incubated at 37 °C with a staining solution containing: 7.2 mM Na₂HPO₄, 2.8 mM NaH₂PO₄, 150 mM NaCl, 1 mM MgCl₂, 3 mM K₃Fe(CN)₆, 3 mM K₄Fe(CN)₆ and 0.3% X-Gal. When the staining appeared the sections were washed twice for 5 min in PBS and mounted in 70% glycerol PBS.

Isolated tibialis anterior muscles of 3 control and 6 EAMG animals were analyzed by immunohistochemistry as described previously (Martínez-Martínez et al., 2007) with the following primary antibodies: mouse anti-rapsyn mAb 1234 (1/500; Sigma, USA) (Bloch and Froehner, 1987); rabbit anti-vesicular acetylcholine transporter (VACHT; 1/500; Sigma, USA); mouse anti-SV2 (directed against synaptic vesicles; 1/5000; DS Hybridoma Bank, USA) and rabbit-anti-sodium channel (III–IV) (1/500; Upstate, USA). The acetylcholine receptor was detected using Alexa 594-conjugated α -BT (1/300; Molecular Probes, Leiden, The Netherlands). All antibodies were diluted in PBS with 2% BSA and incubated at room temperature for 1 h. Washing steps were performed with PBS with 0.05% Triton-X100. Subsequently, the sections were incubated for 1 h at room temperature with the corresponding secondary antibodies: biotinylated donkey anti-mouse Ig (1/400; minimal cross-reaction with rat IgG; Jackson ImmunoResearch, West Grove, USA); Alexa 350-conjugated goat anti-rabbit IgG (1/100; Molecular Probes); Alexa 488-conjugated goat anti-rabbit IgG (1/100 in PBSA; Molecular Probes) or donkey anti-rabbit IgG Alexa-594 (1/100; Molecular Probes). After washing, the biotinylated anti-mouse antibody was stained for 1 h at room temperature with Alexa 488-streptavidin (1/2000; Molecular Probes). Coverslips were mounted with 0.2 M Tris pH = 8 with 80% (v/v) glycerol.

Quantitative immunofluorescence analysis

The amounts of AChR and rapsyn at the neuromuscular junction were analyzed microscopically relative to the presynaptic vesicular acetylcholine transporter (VACHT) as previously described (Losen et al., 2005; Martínez-Martínez et al., 2007). The fluorescence intensities of α -BT labeling correlates well with biochemical measurements of the AChR, with the advantage that the histochemical analysis can be confined to the area of the NMJ without measuring extrajunctional AChR (Losen et al., 2005). Endplate areas were identified as regions of VACHT staining and the mean intensity of VACHT, rapsyn and AChR staining was measured in the corresponding area. The threshold intensity of VACHT staining for defining the margin of NMJ areas were automatically calculated for each picture. The ratios of AChR:VACHT and rapsyn:VACHT were calculated as a relative measure for the postsynaptic rapsyn and AChR concentration. The ratios of voltage gated sodium channel (VGSC) relative to the presynaptic synaptic vesicle protein 2 (SV-2) were calculated as a relative measure for the postsynaptic VGSC concentration. For each experiment, photos of more than 50 endplates per muscle were quantified. The expression of postsynaptic proteins was normalized with measurements in healthy control animals. Changes of postsynaptic protein expression relative to control levels are expressed as difference \pm standard error of the means. Where available, the corresponding reference value from contralateral muscle of the same animal was used and the change of expression was calculated as difference \pm standard deviation of the relative differences.

Two-photon laser scanning microscopy

High power pictures of endplates were taken using a two-photon laser scanning microscope setup as previously described (Martínez-Martínez et al., 2007). For projection of the images the ImageJ software was used.

Electron microscopy

Electron micrographs were taken from endplates of the tibialis anterior muscles of 6 control rats and 3 EAMG rats with unilateral rapsyn silencing treatment. For the α -BT treatment experiment electron micrographs were taken from endplates of the tibialis anterior muscles of 4 sham-treated rats and 3 intramuscular α -BT-treated rats. Anesthetized rats were transcardially perfused as previously described (Losen et al., 2005; Martínez-Martínez et al., 2007). Ultra-thin sections were viewed with Philips CM 100 electron microscope. At least five endplate regions were photographed from each muscle. Pictures were scanned for morphometric analysis using the ImageJ software as described previously (Engel et al., 1976a,b; Losen et al., 2005; Martínez-Martínez et al., 2007).

Statistics

GraphPad Prism 4 was used to perform statistical analyses. Comparison between normally distributed values was performed using a paired or unpaired *t*-test, wherever appropriate. A two-sided probability value <0.05 was considered significant. Values are expressed as means \pm standard deviation (SD) unless stated otherwise.

Results

Rapsyn shRNA reduced rapsyn and AChR protein levels in adult rat muscles

In order to knock-down the expression of rapsyn in the adult muscle, we designed 4 short hairpin oligonucleotides (S1–S4, Table 1) which were cloned into the pSUPER expression vector and initially

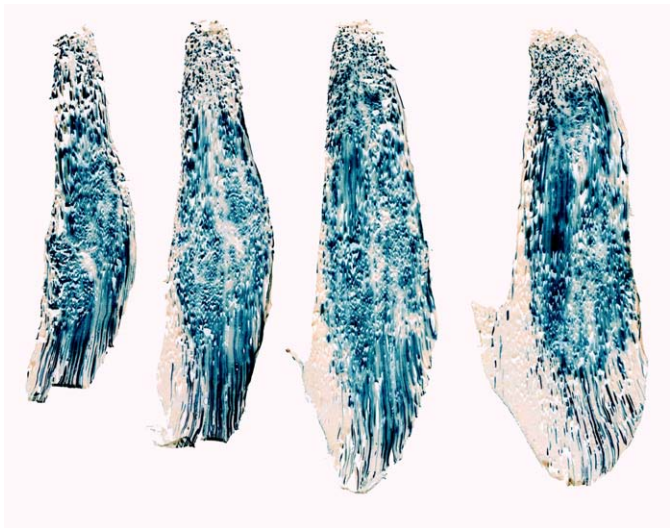


Fig. 1. *In vivo* electroporation of shRNA plasmids. The transfection efficiency was analyzed using X-gal as a substrate for the reporter β -galactosidase. The sections are spaced 500 μ m.

tested *in vitro* by co-transfection with rapsyn-GFP in HEK 293 cells. Following transfection, all 4 pSUPER constructs efficiently reduced the levels of rapsyn-GFP (between 84% and 98%) expression compared to rapsyn-GFP co-transfected with the empty pSUPER vector; the combination of all silencers showed a reduction of rapsyn-GFP levels of 88% ($\pm 9.22\%$, SEM; $p < 0.005$, unpaired *t*-test) (Supplementary Fig. S2).

Subsequently we used electroporation to transfect the shRNA expression vectors into the rat muscles. We pooled equal amounts of shRNA expression vectors S1, S2, S3 and S4, in order to maintain rapsyn silencing while reducing concentrations of each individual plasmid and thereby the contribution of off-target effects (Blow, 2008; Brown and Samarsky, 2006; Hsieh et al., 2004). Because this transfection procedure can lead to transient tissue damage and inflammation (unpublished observations), we used the contralateral muscles as a control. These were injected with a control vector and electroporated using the same protocol. On average, a single electroporation (cf. Losen et al., 2005; Roorda et al., 2005) was not sufficient to reduce rapsyn protein levels at the neuromuscular junction relative to presynaptic VACHT levels at any time point analyzed (2, 4 and 6 weeks; data not shown). However, a few endplates (<1%) from tibialis anterior muscles single-electroporated with silencing vectors showed decreased amounts of rapsyn (Supplementary Fig. S3). Endplates of rat tibialis anterior muscle electroporated with pSUPER empty vector never showed a decrease in rapsyn (not shown) at any time point analyzed, as expected from experiments performed by Kong et al. (2004) with similar vectors. To improve the transfection efficiency we tested repeated electroporations (triple electroporation with 48 h intervals): 8 animals were electroporated in the left tibialis anterior muscle with a combination of pVax- β -galactosidase reporter vector and pSUPER silencing vectors; the contralateral muscles were transfected with pVax- β -galactosidase reporter vector and pSUPER empty vector. Two weeks after transfection, β -gal was present in the majority of muscle cells (>90% of the fibers in the muscle belly, Fig. 1); albeit with widely varying expression levels.

The effect of shRNAs on rapsyn and AChR protein levels was examined in 5 healthy animals and compared to 6 myasthenic rats. Two weeks after the first electroporation and 48 h after the mAb 35 injection for the myasthenic animals the tibialis anterior muscles were isolated. Cryosections from these animals were triple-stained for rapsyn, AChR and for the presynaptic vesicular acetylcholine transporter (VACHT). We used two-photon microscopy to examine the NMJs in detail. Representative endplates of control, silenced and

EAMG muscles are shown in Fig. 2A. Silenced endplates appeared to have reduced amounts of rapsyn and also of AChR compared to endplates in control muscles, while the presynaptic staining of VACHT was unaffected. In EAMG muscles, the AChR and the rapsyn levels in tibialis anterior muscles were strongly reduced. The quantification of immunohistochemical staining of more than 1000 endplates in tibialis anterior muscles of healthy rats confirmed a reduction in the relative concentrations of rapsyn (by $33.2\% \pm 14.5\%$, $p = 0.016$, paired *t*-test) and of AChR (by $33.8\% \pm 13.9\%$, $p = 0.011$, paired *t*-test) as a result of rapsyn-silencing (Figs. 2B, C). This effect was in fact similar to the result of mAb 35 treatment, where rapsyn was reduced by 62.6% ($\pm 11.6\%$, $p < 0.001$ unpaired *t*-test) and the AChR was reduced by 25.5% ($\pm 22.7\%$, $p = 0.062$ unpaired *t*-test) compared to control muscles. The reduction of rapsyn and receptor in rapsyn-silenced muscles was not homogeneous. The distribution of AChR and rapsyn intensities in stained endplates (Figs. 2D, E) shows that some fibers lost more than 50% of rapsyn, while others were unaffected.

Reduced rapsyn expression impairs neuromuscular transmission

To study the effect of unilateral rapsyn-silencing on neuromuscular transmission we measured the compound muscle action potentials (CMAP; using repetitive nerve stimulation at 3 Hz) in tibialis anterior muscles of 8 healthy (control) and 9 myasthenic rats. The safety factor of neuromuscular transmission was challenged by repeated intraperitoneal injections of the AChR antagonist curare until a decrement in the response of the CMAP was observed. The stimulations and CMAP measurements were performed bilaterally and simultaneously in the tibialis anterior muscles in order to detect differences between the non-silenced and the rapsyn-silenced leg. The resistance against curare was used as an indirect, albeit non-linear, measure for the safety factor of neuromuscular transmission. Representative examples of CMAP measurements of control, silenced and EAMG animals are shown in Figs. 3A–C), and the results of all animals are summarized in Fig. 3D). In control muscles a cumulative dose of 11.4 μ g ($\pm 3.1 \mu$ g) of curare was required to induce a reproducible decremental response of the CMAP (>10%). By contrast, the contralateral rapsyn-silenced muscles were significantly less resistant against curare (8.8 μ g $\pm 3.1 \mu$ g, $p = 0.006$ paired *t*-test). Since rapsyn loss is also observed in experimental autoimmune myasthenia gravis (EAMG) models (cf. Losen et al., 2005; Martínez-Martínez et al., 2007) we performed identical electromyography measurements in a passive transfer model of MG with the anti-AChR mAb 35. EAMG was induced in 9 rats (12 days after sham electroporation of the tibialis anterior muscles with control plasmids). Within 48 h all animals had clear clinical signs of EAMG (score of ++ in each animal). Decrementing responses could be demonstrated without curare injections (4 out of 9 animals) while in the other animals very low curare doses were sufficient to induce decrement (between 0.25 and 2.5 μ g; on average 0.6 μ g $\pm 0.6 \mu$ g, $n = 9$, $p < 0.001$ compared to non-silenced control muscles). On the basis of these measurements, the neuromuscular transmission defect caused by mAb 35 alone was significantly more severe than caused by rapsyn-silencing ($p < 0.001$).

Rapsyn silencing causes increased folding of the postsynaptic membrane

Since the reduction of the safety factor of neuromuscular transmission after rapsyn-silencing and mAb 35 did not correlate to synaptic AChR expression, we speculated that ultrastructural differences were the underlying cause for the observed effects. Therefore, we performed electron microscopic observations and morphometric analysis on tibialis anterior muscles of 3 EAMG and 6 control rats 2 weeks after unilateral rapsyn-silencing.

Indeed, the silencing of rapsyn altered the structure of the NMJ (Fig. 4B). There was an increase in the average length of the postsynaptic membrane compared to that of control muscles (Fig. 4A). Quantitative

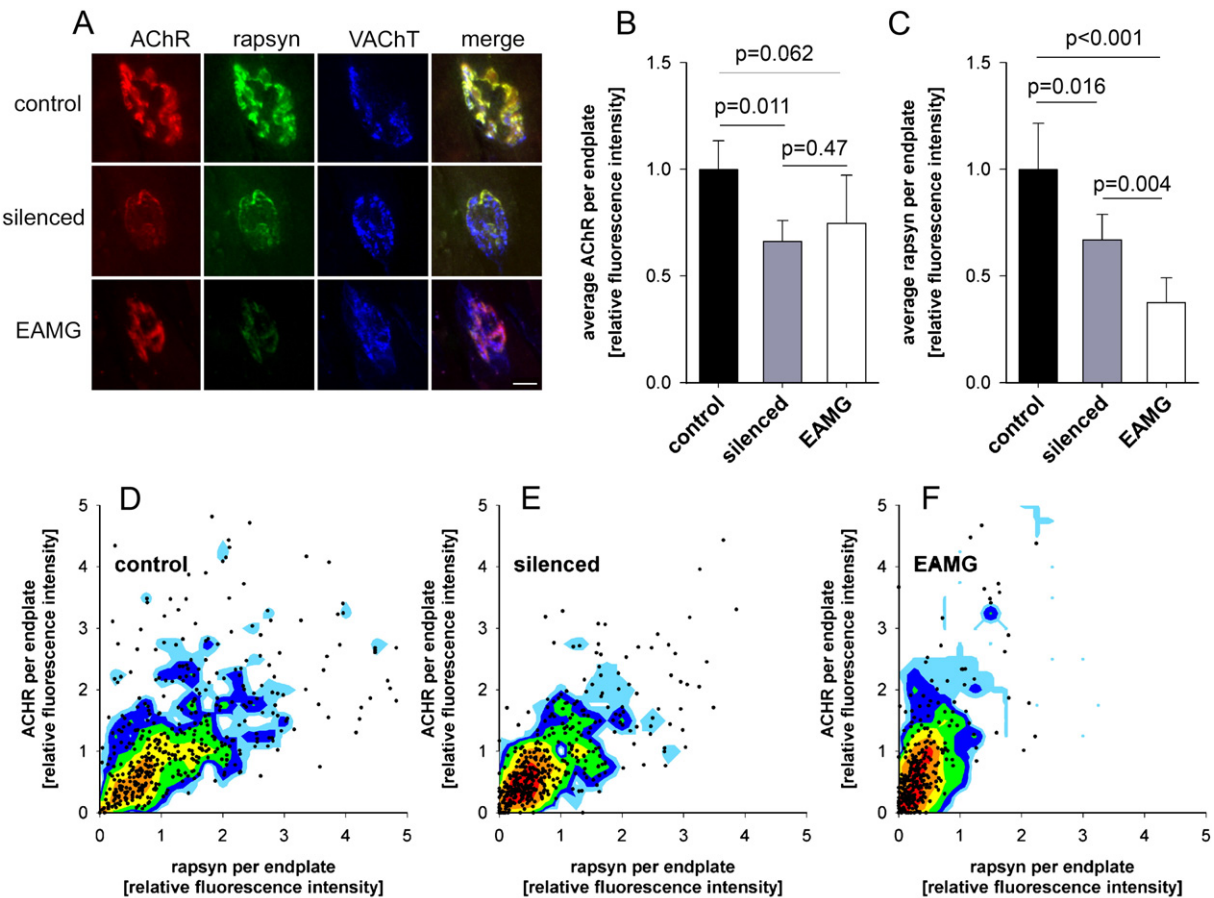


Fig. 2. Two-photon laser scanning microscopy images of representative endplates and quantitative immunohistochemistry analysis. Muscle sections were triple stained for AChR (red), rapsyn (green) and the presynaptic protein VAcHT (blue) as a reference. (A) In rapsyn-silenced muscles most endplates showed reduced AChR and rapsyn levels relative to VAcHT. Passive transfer of anti-AChR antibodies caused a similar reduction of these proteins. Scale bar is 10 μ m. Measurement of fluorescence intensities of AChR (B) and rapsyn (C) relative to VAcHT staining of endplates in 5 control, 5 silenced and 6 EAMG muscles. Error bars indicate the standard deviation. At least 120 endplates were analyzed per muscle. Staining intensities were normalized to the average intensities of control endplates. The distribution of normalized staining intensities of individual endplates is shown for control muscles (D), silenced muscles (E) and EAMG muscles (F).

morphometric analysis confirmed a significantly increased length of the postsynaptic membrane relative to the presynaptic membrane (folding index; Fig. 4D). The folding index showed considerable variation in the tibialis anterior muscle, which is possibly due to differential specialization of the postsynaptic membrane in type I and type II fibers (Pachter and Eberstein, 1984, 1986). The area of postsynaptic folds was increased and the nerve terminal size was slightly, but significantly decreased in rapsyn-silenced muscles (Table 2; $p < 0.05$). Although it appeared that some postsynaptic folds were not directly adjacent to nerve terminals (e.g. in Fig. 4B), analysis of serial sections of endplates showed that such areas were also connected to over or underlying nerve boutons (Supplementary Fig. S4). As expected, endplates in the EAMG muscles showed the typical reduction of the folding index (Fig. 4C) compared to control muscles. Interestingly, also a reduction of the nerve terminal bouton size was observed in rapsyn-silenced muscles, suggesting the possibility that rapsyn is involved in retrograde signaling from the muscle to the nerve.

Rapsyn shRNA increased voltage gated sodium channel protein levels in adult rat muscles

In addition to the AChRs the postsynaptic membrane contains a high density of voltage gated sodium channels (VGSCs). VGSCs have a postsynaptic localization at the troughs of folds where they are 10 times as concentrated as in the membrane far from the NMJs (Flucher and Daniels, 1989). To study how the silencing of rapsyn affected the

concentration of VGSCs in the increased folding of the postsynaptic membrane, we performed quantitative immunofluorescence analysis on the muscle fibers (as described above for rapsyn and AChR). Cryosections of the isolated tibialis anterior muscles were double-stained for VGSCs and the presynaptic marker SV-2. Endplates in rapsyn-silenced tibialis anterior muscles showed an increase in the concentration of VGSC compared to control muscles (Fig. 5A). The quantification of immunohistochemical staining of endplates in rapsyn-silenced tibialis anterior muscles confirmed an increase in the relative concentrations of VGSCs (by $26.1 \pm 24.2\%$, $p = 0.032$, paired t -test) compared to control endplates. In EAMG tibialis anterior muscles VGSCs were reduced (by $27.9 \pm 7.8\%$, $p < 0.001$ unpaired t -test) compared to control muscles (Fig. 5B). In conclusion, the VGSC levels correlated well with the folding index and folding area of the postsynaptic membrane.

Bungarotoxin treatment increases both the presynaptic and the postsynaptic membrane lengths

The effect of rapsyn-silencing on endplate structure could have been due to an off-target effect, a direct effect of rapsyn loss, or to an indirect effect caused by reduction of the number of AChRs per endplate which follows rapsyn silencing. In order to test the latter possibility, tibialis muscles were directly injected with repeated doses of α -BT for a period of 15 days to block the AChR activity. To study how this procedure affected the ultrastructure of the neuromuscular junctions, we performed electron microscopic observations and

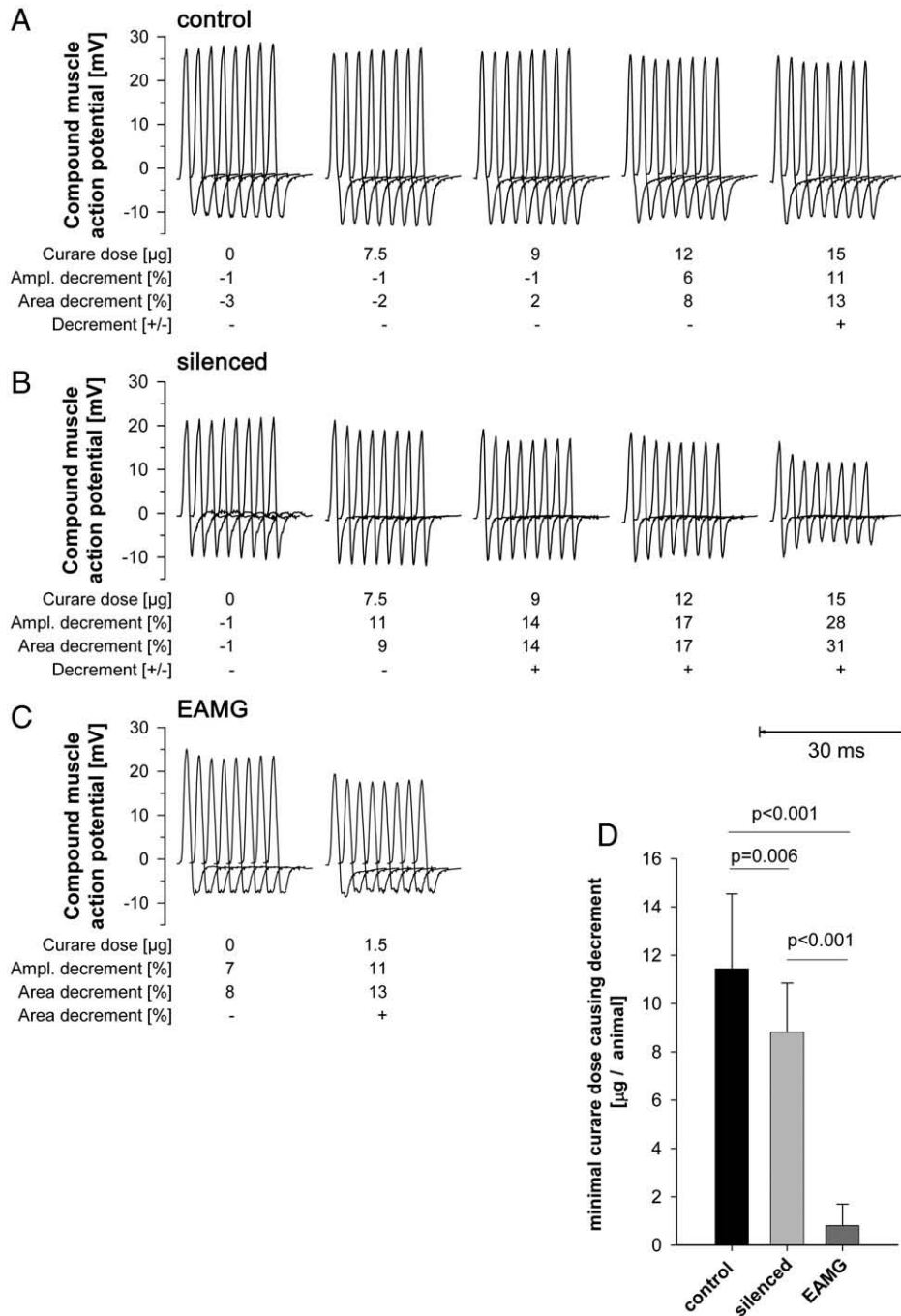


Fig. 3. Measurement of curare sensitivity of neuromuscular transmission. Compound muscle action potentials of the transfected tibialis anterior muscles were measured bilaterally during repetitive nerve stimulation. Doses of curare were injected repeatedly with 10 min intervals until a reproducible decremental response was observed in both muscles. The minimal cumulative curare dose that caused decrement in control muscles (an example is shown in A) was always higher than in the contralateral rapsyn-silenced muscles (example in B). In EAMG animals decrement could be induced without or with very low doses of curare (C). (D) Average minimal cumulative curare dose that induced at least 10% decrement of the CMAP in 5 control muscles, 5 silenced muscles and muscles of 5 EAMG animals. Error bars indicate the standard deviation.

morphometric analysis in 4 saline-treated and 3 α -BT-treated animals. Compared with saline treatment, the endplates showed morphological abnormalities after the treatment with α -BT (Fig. 6). The most remarkable abnormality was the significant increase in length of the pre- as well as the postsynaptic membrane ($p < 0.05$; unpaired *t*-test) (Table 3). As such, there is an increased contact area between the pre- and the postsynaptic membranes, which is observed in 99 out of 150 regions (Figs. 6B, C). Because of the increase of both the presynaptic and the postsynaptic membrane lengths, the ratio of postsynaptic to presynaptic membrane length was not significantly

different ($p = 0.81$, unpaired *t*-test; Table 3). A change of the nerve bouton size was not observed under these conditions. In conclusion, the postsynaptic changes observed after α -BT treatment were very similar to those observed after rapsyn silencing, while the presynaptic alterations were not identical.

Discussion

In this study we analyzed the effect of reduced rapsyn expression levels in the adult neuromuscular junction by shRNA. Reduced rapsyn

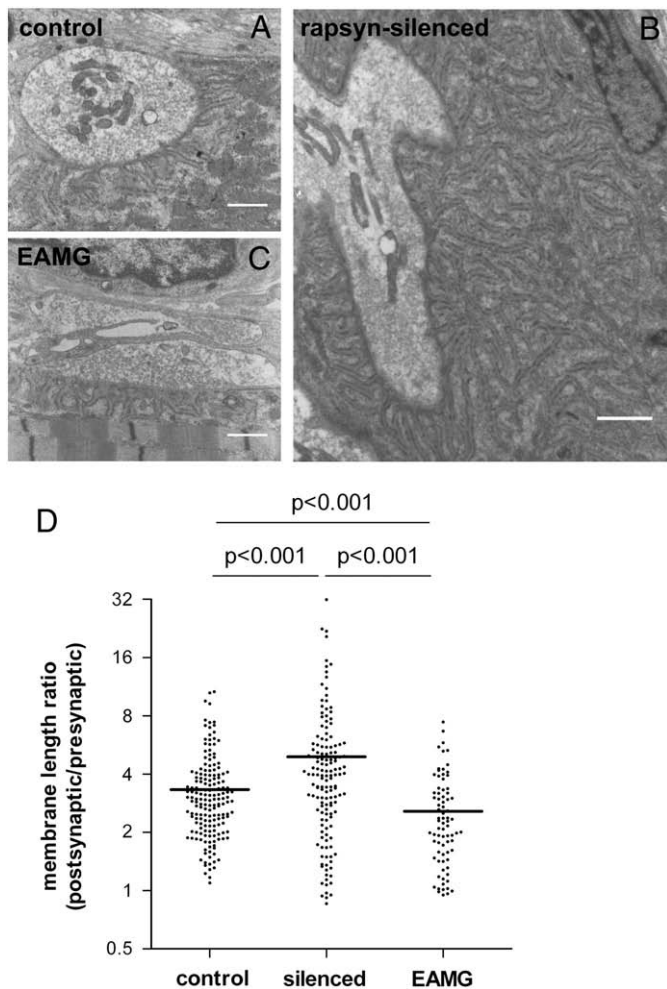


Fig. 4. Electron microscopic analysis of endplate morphology (scale bar 1 μm). (A) Normal endplate region in a control muscle. (B) Endplates in the contralateral rapsyn-silenced muscle of the same animal showed varying degrees of increased secondary folds. Shown is a conspicuous example. (C) Passive transfer of anti-AChR antibodies causes widening of the synaptic cleft and a reduction of postsynaptic folding. (D) Quantitative morphometric analysis of the postsynaptic folding index. Each data point represents the ratio of the total postsynaptic membrane length (including primary gutter and secondary clefts) and the presynaptic membrane of one or two nerve corresponding nerve boutons (folding index). Note that the ordinate is a logarithmic scale. Other parameters of the quantitative morphometric analysis are presented in Table 2.

levels led to reduction of AChR and a moderate impairment of the safety factor of neuromuscular transmission. Conversely, the VGSCs, which are located in the troughs of the postsynaptic membrane, were increased in silenced muscles. Surprisingly, postsynaptic membrane folding was markedly increased. Together with the increase in VGSC levels this probably represents a compensatory mechanism to protect neuromuscular transmission since the density

of sodium channels in the postsynaptic folds determines the firing threshold and safety factor of the neuromuscular transmission (Wood and Slater, 1997).

For the interpretation of the results it is important to consider off-target effects of the shRNA electroporation procedure (Jackson et al., 2003). Off target effects can be caused by the transfection method, double-stranded RNA-induced inflammation and RISC-dependent effects. As a control for the transfection method we electroporated the contralateral tibialis anterior muscles in each animal with a control plasmid and used these muscles as a reference in the experiments. Because of multiple injections and electroporation, muscles were subjected to transient damage and inflammation, and were thus not completely normal. Because plasmid DNA and not dsRNA was used for the transfection, activation of the interferon response via Toll like receptor 3 (Reynolds et al., 2006; Sledz et al., 2003) was less likely to be involved. In order to reduce the chance of possible sequence dependent off-target responses we used the minimal effective amount of 4 different shRNA expression plasmids, which all target rapsyn, but not likely the same potential off-target protein. Moreover, compared to the results using shRNA against rapsyn, we found similar structural changes of the postsynaptic membrane when we blocked the AChR with α -BT. Since rapsyn and AChR activity are closely coupled, this effect is not likely due to off-target effects of the shRNAs.

The finding that rapsyn negatively influences postsynaptic folding may seem contradictory to the data obtained with the rapsyn knock-out model (Gautam et al., 1995) and findings in biopsies of congenital myasthenic syndromes with rapsyn mutations. Indeed, mutations within the *RAPSN* gene have been shown to underlie a high proportion of AChR deficiency syndromes (Burke et al., 2003; Dunne and Maselli, 2003; Ios et al., 2004; Maselli et al., 2003a; Muller et al., 2003; Ohno et al., 2002, 2003). Endplates of patients with the N88K rapsyn mutation contain a reduced number of postsynaptic folds (Ohno et al., 2002, 2003), which could lead to a reduction of the safety factor of the neuromuscular transmission (Ruff and Lennon, 1998, 2008). However, the N88K mutation does not only lead to a very low rapsyn expression, but also impairs its self-aggregation and AChR clustering (Cossins et al., 2006). Conversely, in our experiments, rapsyn was silenced in adult rats and the rapsyn protein levels were reduced, without affecting the intrinsic properties of the protein. The distinct morphology of rapsyn-silenced endplates and the mild impairment of the safety factor of neuromuscular transmission in rapsyn-silenced muscles suggest that the reduction of rapsyn expression is not the primary cause of the disease in CMS associated with N88K rapsyn mutations, which would rather be caused by the alteration of rapsyn function. In rapsyn knock-out mice, already the initial steps of postsynaptic differentiation are blocked, so the lack of postsynaptic folding in the animals is likely due to rapsyn-dependent steps of early subsynaptic gene expression that is also affected in agrin and MuSK knock-out mice (Gautam et al., 1999). It will be interesting to study the ultrastructure of heterozygous *rapsyn*^{+/-} mice and in CMS patients with the homozygous *RAPSN*-promoter mutation -38A/G which reduces rapsyn expression (Ohno et al., 2003).

Table 2
Morphometric analysis of endplates in rapsyn-silenced, EAMG and control muscles*.

	Regions analyzed ^a	Animals per group	Nerve bouton area [μm^2]	Presynaptic membrane length [μm]	Postsynaptic area [μm^2]	Postsynaptic membrane length [μm]	Membrane length ratio (postsynaptic/presynaptic)
Control	197	6	2.8 \pm 0.12	3.2 \pm 0.38	6.52 \pm 4.44	14.4 \pm 1.62	3.3 \pm 0.17 ^c
Silenced	182	6	2.3 \pm 0.15 ^b	3.9 \pm 0.50	8.30 \pm 7.60 ^b	37.4 \pm 5.14	4.9 \pm 0.52 ^c
EAMG	92	3	2.7 \pm 0.11	2.2 \pm 0.91	6.89 \pm 4.83	8.8 \pm 0.63 ^c	2.4 \pm 0.27 ^c

Other differences in this table are not significant ($p > 0.05$).

* Mean \pm SE.

^a A region here refers to an area of one synaptic bouton and the adjacent postsynaptic membrane.

^b Significantly different from control endplates ($p < 0.05$).

^c Significantly different from all other conditions ($p < 0.05$).

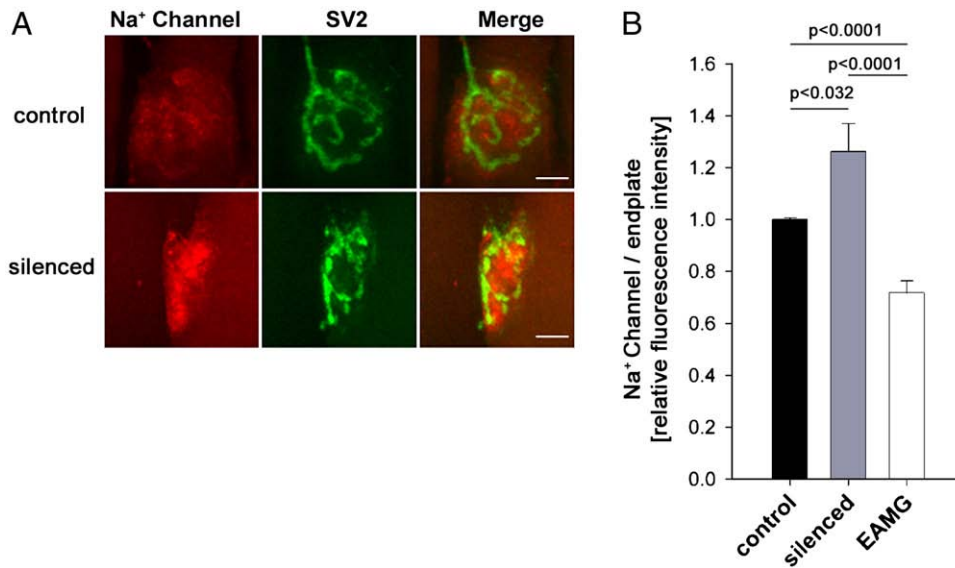


Fig. 5. Analysis of postsynaptic VGSC expression. (A) Confocal microscopy images of representative endplates. Muscle sections were stained for sodium channel (red), and the presynaptic vesicle protein 2 (SV-2; green) as a reference. In rapsyn-silenced muscles most endplates showed increased sodium channel levels compared to control endplates. Scale bar is 10 μ m. (B) Measurement of fluorescence intensities of VGSCs relative to presynaptic SV-2 staining in control, rapsyn-silenced and EAMG muscles. Error bars correspond to the standard deviations. Staining intensities were normalized to the average intensities of control endplates.

In experimental autoimmune MG, rapsyn is lost concomitantly with the AChR (Losen et al., 2005; Martínez-Martínez et al., 2007). Since reduced rapsyn expression can possibly lead to a neuromuscular transmission defect by itself, we addressed the issue of the role of rapsyn reduction in autoimmune MG. Because AChR expression levels were similarly reduced in EAMG and silenced muscles, we could compare the respective impacts of reduced postsynaptic membrane folding and membrane attack complex on neuromuscular transmission. For this purpose, electromyography measurements were performed in the presence of increasing doses of curare to evaluate the neuromuscular safety factor. Despite similarly reduced synaptic rapsyn and AChR levels, the 'safety factor' expressed as the resistance to curare, in EAMG muscles was much lower than in rapsyn-silenced muscles. These data confirm previous observations (Ruff and Lennon, 1998, 2008) suggesting that not only AChR loss, but also the loss of postsynaptic folds with VGSC and/or the presence of membrane attack complex strongly worsened the neuromuscular transmission defects in EAMG. The mechanism of postsynaptic folding reduction in EAMG is a concerted action of cross-linking antibodies and complement activation (Losen et al., 2008). Although complement-mediated membrane attack can contribute to the severe neuromuscular transmission defect in EAMG muscles (as a result of its depolarizing

effect), it is not sufficient to induce decrement by itself. We have previously shown that increased rapsyn expression prevents AChR modulation and efficiently protects synapses against complement activation (Losen et al., 2005). Therefore, it can be argued that increased postsynaptic folding in rapsyn-silenced muscles may serve to compensate for the loss of rapsyn–AChR clusters at the postsynaptic membrane, which would otherwise lead to a great reduction of the safety factor, as we presently observed in EAMG muscle. This is in line with previous observations that the complexity of postsynaptic folding of the neuromuscular junction can increase the safety factor (Ruff and Lennon, 1998; Wood and Slater, 1997, 2001). In this respect, it is interesting to note that the human neuromuscular junction has used the same strategy to compensate for low AChR expression compared to other species, which in turn have less complex postsynaptic folding (Wood and Slater, 2001). It seems possible, that in MG, because of the reduction of the levels of AChR and rapsyn, there is also a tendency for an increase in the level of endplate VGSC and of the extent of postsynaptic folding, but that this is counteracted by autoimmune-induced damage to the endplate. Such a regulation seems likely, since also rapsyn and AChR mRNA expression are upregulated in EAMG to compensate for rapsyn and AChR loss (Asher et al., 1993).

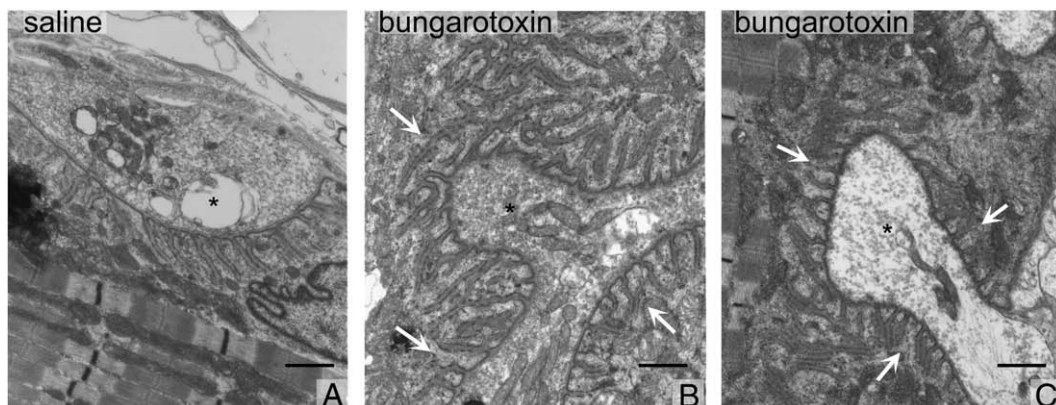


Fig. 6. Electron microscopic examination of neuromuscular junctions in saline-treated (A) and α -BT-treated (B and C) tibialis anterior muscles. Arrows indicate an enlarged contact area between the pre- and the postsynaptic membranes; stars indicate the nerve boutons; scale bars are 1 μ m.

Table 3
Morphometric analysis of endplates following α -BT treatment*.

	Regions analyzed ^a	Nerve bouton area [μm^2]	Presynaptic membrane [μm]	Postsynaptic area [μm^2]	Postsynaptic membrane [μm]	Membrane length ratio (postsynaptic/presynaptic)
Saline-treated	139	2.4 \pm 1.5	8.0 \pm 5.2	7.75 \pm 4.50	32.7 \pm 18.9	4.5 \pm 2.0
α -BT-treated	150	2.9 \pm 1.8	12.2 \pm 10.5 ^b	11.98 \pm 15.29 ^b	55.2 \pm 53.2 ^b	4.6 \pm 2.5

Other differences in this table are not significant ($p > 0.05$).

* Mean \pm SE.

^a A region here refers to an area of one or more synaptic boutons.

^b Significantly different from saline-treated control endplates ($p < 0.05$).

So far, very little is known about the mechanisms that regulate postsynaptic folding. The increase of postsynaptic folding is possibly mediated via the balance between acetylcholine and agrin, which have been identified as key factors in synapse differentiation. Since agrin is thought to counteract the ACh-dependent dispersal of AChR clusters in embryonic muscle (Lin et al., 2005; Misgeld et al., 2005), we investigated the possibility that postsynaptic membrane folding was regulated via AChR activation by ACh. Alternatively, one could postulate that the protein levels of rapsyn and AChR could directly determine membrane folding, independently of ACh, electrical activity or ensuing changes of intracellular concentrations of Ca^{2+} and Na^+ . To answer this question, α -BT was directly injected into the tibialis muscles of rats in order to block AChR activity. Subsequently, we analyzed the effect of AChR blocking by electron microscopy. This treatment also led to a marked increase in postsynaptic membrane area and length, suggesting that AChR activity is indeed correlated to postsynaptic membrane structure. Because the contact area between the muscle and the nerve boutons was also increased, the folding index was not changed. The different presynaptic manifestations of rapsyn silencing versus α -BT-treatment might reflect the degree of AChR blocking.

Interestingly, recent studies showed that α -BT does not only block the AChR, but also induces rapid disaggregation of AChR/rapsyn clusters, without affecting synaptic AChR protein levels (Brockhausen et al., 2008). Therefore, it is possible, that also the α -BT-induced increase of postsynaptic membrane folding is mediated via rapsyn. Since rapsyn concentration and AChR activity are closely correlated, we cannot conclude which of these two proteins are responsible for the observed morphological changes at the NMJ.

Of course, these results do not exclude the possibility that rapsyn expression can also modulate synapse morphology via other molecules. It has been described that in addition to its role in AChR anchoring to the cytoskeleton, rapsyn specifically interacts with beta-catenin, which is involved in NMJ presynaptic differentiation and function (Li et al., 2008; Zhang et al., 2007). Interestingly, we also found presynaptic changes in rapsyn-silenced muscles. Furthermore, rapsyn interaction with calpain, a calcium-dependent protease, has been shown to stabilize AChR clusters at the NMJ (Chen et al., 2007). Unfortunately, nothing is known yet about the effect of these interactions at the ultrastructural level and the molecular mechanism by which rapsyn exerts its effect on pre- and postsynaptic differentiation will require further investigation. The described results allow the conclusion that agrin does not increase postsynaptic folding via increased rapsyn/AChR interaction.

Our results are compatible with the hypothesis that ACh negatively and agrin positively regulate synapse differentiation (Lin et al., 2005; Misgeld et al., 2005). As an extension to this hypothesis, we propose that ACh and agrin not only affect AChR-rapsyn clustering, but also VGSC accumulation and membrane folding. Interestingly, neuropathology has already provided us with examples where increased synaptic complexity is found. In some cases of Lambert–Eaton myasthenic syndrome (LEMS) increased folding of the postsynaptic membrane (Santa et al., 1972) or increased nerve muscle contact (Hesselmans et al., 1992) occurs. LEMS is an autoimmune disease in which antibodies interfere with presynaptic calcium channel function

causing a reduction of calcium-dependent ACh release (Santa et al., 1972). Limb immobilization, which causes a decrease of neuronal activity, provides another example of increased NMJ complexity. The main features of these NMJs are terminal sprouting and ultrastructural remodeling sometimes corresponding to large expanses of postsynaptic folds without associated nerve terminals (Pachter and Eberstein, 1984; Pachter and Eberstein, 1986). These, and other examples of increased complexity (Gomez et al., 1996; Maselli et al., 2003b; Sroka et al., 1975) might be explained by the considerable ability of the NMJ to respond to defects in some of its components by compensatory enhancement of others.

Pre- and postsynaptic components change during development and may show plasticity in response to injury or disease. It has been suggested that the structure and molecular organization of the postsynaptic apparatus takes an excess of the released transmitter from the nerve, helping to ensure that every nerve impulse normally triggers a muscle action potential with a very small chance of failure. The concept of safety factor for neuromuscular transmission describes this excess (Martin, 1994; Wood and Slater, 1995, 1997, 2001). It is of interest that a modest reduction of rapsyn expression already causes substantial changes, showing that the amount of rapsyn is critically related to the AChR levels and to the structure of the endplate. In all analyzed conditions, rapsyn and AChR levels were strongly correlated. This is in line with previous observations performed at sites undergoing synapse elimination, where rapsyn loss was parallel to AChR loss (Culican et al., 1998). The present study suggests that rapsyn determines AChR density at the adult NMJ, and supports the hypothesis that functional AChR and rapsyn clusters negatively regulate postsynaptic folding. Finally, the results indicate a very dynamic subsynaptic machinery in adult NMJs that can rapidly extend postsynaptic folds or produce new ones.

Acknowledgments

We would like to thank Jean Cartaud from the Institut Jacques Monod for the rapsyn–GFP construct and Reuven Agami from the Netherlands Cancer Institute for providing the pSUPER vector and advice for cloning the silencing constructs. P.M.-M was supported by grants from the Prinses Beatrix Fonds (project: MAR03-0115) and L'Association Française contre les Myopathies. We would like to thank Robert van Os, Phillip Becker and Joost van den Broeck for their help with the quantitative morphometry analysis and Eline van der Esch for her excellent technical assistance.

Appendix A. Supplementary data

Supplementary data associated with this article can be found, in the online version, at doi:10.1016/j.nbd.2009.03.008.

References

- Asher, O., et al., 1993. Increased gene expression of acetylcholine receptor and myogenic factors in passively transferred experimental autoimmune myasthenia gravis. *J. Immunol.* 151, 6442–6450.
- Bezakova, G., et al., 2001. Neural agrin controls acetylcholine receptor stability in skeletal muscle fibers. *Proc. Natl. Acad. Sci. U. S. A.* 98, 9924–9929.

- Bloch, R.J., Froehner, S.C., 1987. The relationship of the postsynaptic 43K protein to acetylcholine receptors in receptor clusters isolated from cultured rat myotubes. *J. Cell. Biol.* 104, 645–654.
- Blow, N., 2008. RNAi technologies: a screen whose time has arrived. *Nat. Methods* 5, 361–366.
- Brockhausen, J., et al., 2008. Neural agrin increases postsynaptic ACh receptor packing by elevating rapsyn protein at the mouse neuromuscular synapse. *Dev. Neurobiol.* 68, 1153–1169.
- Brown, K., Samarsky, D., 2006. RNAi off-targeting: light at the end of the tunnel. *Journal of RNAi and Gene Silencing* 2, 175–177.
- Brummelkamp, T.R., et al., 2002. A system for stable expression of short interfering RNAs in mammalian cells. *Science* 296, 550–553.
- Burke, G., et al., 2003. Rapsyn mutations in hereditary myasthenia: distinct early- and late-onset phenotypes. *Neurology* 61, 826–828.
- Chen, F., et al., 2007. Rapsyn interaction with calpain stabilizes AChR clusters at the neuromuscular junction. *Neuron* 55, 247–260.
- Cossins, J., et al., 2006. Diverse molecular mechanisms involved in AChR deficiency due to rapsyn mutations. *Brain* 129, 2773–2783.
- Culican, S.M., et al., 1998. Axon withdrawal during synapse elimination at the neuromuscular junction is accompanied by disassembly of the postsynaptic specialization and withdrawal of Schwann cell processes. *J. Neurosci.* 18, 4953–4965.
- De Baets, M., et al., 2003. Immunoregulation in experimental autoimmune myasthenia gravis—about T cells, antibodies, and endplates. *Ann. N.Y. Acad. Sci.* 998, 308–317.
- DeChiara, T.M., et al., 1996. The receptor tyrosine kinase MuSK is required for neuromuscular junction formation in vivo. *Cell* 85, 501–512.
- Dunne, V., Maselli, R.A., 2003. Identification of pathogenic mutations in the human rapsyn gene. *J. Hum. Genet.* 48, 204–207.
- Elbashir, S.M., et al., 2001. Duplexes of 21-nucleotide RNAs mediate RNA interference in cultured mammalian cells. *Nature* 411, 494–498.
- Engel, A.G., Sine, S.M., 2005. Current understanding of congenital myasthenic syndromes. *Curr. Opin. Pharmacol.* 5, 308–321.
- Engel, A.G., et al., 1976a. Experimental autoimmune myasthenia gravis: a sequential and quantitative study of the neuromuscular junction ultrastructure and electrophysiological correlations. *J. Neuropathol. Exp. Neurol.* 35, 569–587.
- Engel, A.G., et al., 1976b. The motor end plate in myasthenia gravis and in experimental autoimmune myasthenia gravis. A quantitative ultrastructural study. *Ann. N.Y. Acad. Sci.* 274, 60–79.
- Flucher, B.E., Daniels, M.P., 1989. Distribution of Na⁺ channels and ankyrin in neuromuscular junctions is complementary to that of acetylcholine receptors and the 43 kd protein. *Neuron* 3, 163–175.
- Gautam, M., et al., 1999. Distinct phenotypes of mutant mice lacking agrin, MuSK, or rapsyn. *Brain Res. Dev. Brain Res.* 114, 171–178.
- Gautam, M., et al., 1996. Defective neuromuscular synaptogenesis in agrin-deficient mutant mice. *Cell* 85, 525–535.
- Gautam, M., et al., 1995. Failure of postsynaptic specialization to develop at neuromuscular junctions of rapsyn-deficient mice. *Nature* 377, 232–236.
- Gervasio, O.L., et al., 2007. Developmental increase in the amount of rapsyn per acetylcholine receptor promotes postsynaptic receptor packing and stability. *Dev. Biol.* 305, 262–275.
- Gervasio, O.L., Phillips, W.D., 2005. Increased ratio of rapsyn to ACh receptor stabilizes postsynaptic receptors at the mouse neuromuscular synapse. *J. Physiol.* 562, 673–685.
- Gomez, C.M., et al., 1996. A beta-subunit mutation in the acetylcholine receptor channel gate causes severe slow-channel syndrome. *Ann. Neurol.* 39, 712–723.
- Hantai, D., et al., 2004. Congenital myasthenic syndromes. *Curr. Opin. Neurol.* 17, 539–551.
- Hesselmans, L.F., et al., 1992. Secondary changes of the motor endplate in Lambert–Eaton myasthenic syndrome: a quantitative study. *Acta Neuropathol.* 83, 202–206.
- Hoedemaekers, A., et al., 1998. Role of the target organ in determining susceptibility to experimental autoimmune myasthenia gravis. *J. Neuroimmunol.* 89, 131–141.
- Hoedemaekers, A., et al., 1997a. Age- and sex-related resistance to chronic experimental autoimmune myasthenia gravis (EAMG) in Brown Norway rats. *Clin. Exp. Immunol.* 107, 189–197.
- Hoedemaekers, A., et al., 1997b. Age-related susceptibility to experimental autoimmune myasthenia gravis: immunological and electrophysiological aspects. *Muscle Nerve* 20, 1091–1101.
- Hsieh, A.C., et al., 2004. A library of siRNA duplexes targeting the phosphoinositide 3-kinase pathway: determinants of gene silencing for use in cell-based screens. *Nucleic Acids Res.* 32, 893–901.
- Ioos, C., et al., 2004. Congenital myasthenic syndrome due to rapsyn deficiency: three cases with arthrogryposis and bulbar symptoms. *Neuropediatrics* 35, 246–249.
- Jackson, A.L., et al., 2003. Expression profiling reveals off-target gene regulation by RNAi. *Nat. Biotechnol.* 21, 635–637.
- Janssen, S.P., et al., 2008. Immunosuppression of experimental autoimmune myasthenia gravis by mycophenolate mofetil. *J. Neuroimmunol.* 201–202, 111–120.
- Kim, N., et al., 2008. Lrp4 is a receptor for Agrin and forms a complex with MuSK. *Cell* 135, 334–342.
- Kimura, J., 2001. *Electrodiagnosis in Diseases of Nerve and Muscle: Principles and Practice*. Oxford University Press, Oxford.
- Kong, X.C., et al., 2004. Inhibition of synapse assembly in mammalian muscle in vivo by RNA interference. *EMBO Rep.* 5, 183–188.
- Li, X.M., et al., 2008. Retrograde regulation of motoneuron differentiation by muscle beta-catenin. *Nat. Neurosci.* 11, 262–268.
- Lin, W., et al., 2005. Neurotransmitter acetylcholine negatively regulates neuromuscular synapse formation by a Cdk5-dependent mechanism. *Neuron* 46, 569–579.
- Losen, M., et al., 2008. Treatment of myasthenia gravis by preventing acetylcholine receptor modulation. *Ann. N.Y. Acad. Sci.* 1132, 174–179.
- Losen, M., et al., 2005. Increased expression of rapsyn in muscles prevents acetylcholine receptor loss in experimental autoimmune myasthenia gravis. *Brain* 128, 2327–2337.
- Marchand, S., et al., 2002. Rapsyn escorts the nicotinic acetylcholine receptor along the exocytic pathway via association with lipid rafts. *J. Neurosci.* 22, 8891–8901.
- Martin, A.R., 1994. Amplification of neuromuscular-transmission by postjunctional folds. *Proc. R. Soc. Lond., B Biol. Sci.* 258, 321–326.
- Martínez-Martínez, P., et al., 2007. Overexpression of rapsyn in rat muscle increases acetylcholine receptor levels in chronic experimental autoimmune myasthenia gravis. *Am. J. Pathol.* 170, 644–657.
- Maselli, R.A., et al., 2003a. Rapsyn mutations in myasthenic syndrome due to impaired receptor clustering. *Muscle Nerve* 28, 293–301.
- Maselli, R.A., et al., 2003b. Presynaptic failure of neuromuscular transmission and synaptic remodeling in EA2. *Neurology* 61, 1743–1748.
- Misgeld, T., et al., 2005. Agrin promotes synaptic differentiation by counteracting an inhibitory effect of neurotransmitter. *Proc. Natl. Acad. Sci. U. S. A.* 102, 11088–11093.
- Molenaar, P.C., et al., 1991. A non-immunogenic myasthenia gravis model and its application in a study of transsynaptic regulation at the neuromuscular junction. *Eur. J. Pharmacol.* 196, 93–101.
- Muller, J.S., et al., 2003. Rapsyn N88K is a frequent cause of congenital myasthenic syndromes in European patients. *Neurology* 60, 1805–1810.
- Nitkin, R.M., et al., 1987. Identification of agrin, a synaptic organizing protein from Torpedo electric organ. *J. Cell. Biol.* 105, 2471–2478.
- Ohno, K., et al., 2002. Rapsyn mutations in humans cause endplate acetylcholine-receptor deficiency and myasthenic syndrome. *Am. J. Hum. Genet.* 70, 875–885.
- Ohno, K., et al., 2003. E-box mutations in the RAPSN promoter region in eight cases with congenital myasthenic syndrome. *Hum. Mol. Genet.* 12, 739–748.
- Pachter, B.R., Eberstein, A., 1984. Neuromuscular plasticity following limb immobilization. *J. Neurocytol.* 13, 1013–1025.
- Pachter, B.R., Eberstein, A., 1986. The effect of limb immobilization and stretch on the fine structure of the neuromuscular junction in rat muscle. *Exp. Neurol.* 92, 13–19.
- Reynolds, A., et al., 2006. Induction of the interferon response by siRNA is cell type- and duplex length-dependent. *RNA* 12, 988–993.
- Roorda, B.D., et al., 2005. DGAT1 overexpression in muscle by in vivo DNA electroporation increases intramyocellular lipid content. *J. Lipid Res.* 46, 230–236.
- Ruff, R.L., Lennon, V.A., 1998. End-plate voltage-gated sodium channels are lost in clinical and experimental myasthenia gravis. *Ann. Neurol.* 43, 370–379.
- Ruff, R.L., Lennon, V.A., 2008. How myasthenia gravis alters the safety factor for neuromuscular transmission. *J. Neuroimmunol.* 201–202, 13–20.
- Santa, T., et al., 1972. Histometric study of neuromuscular junction ultrastructure. II. Myasthenic syndrome. *Neurology* 22, 370–376.
- Seybold, M.E., et al., 1976. Experimental autoimmune myasthenia: clinical, neurophysiological, and pharmacologic aspects. *Ann. N.Y. Acad. Sci.* 274, 275–282.
- Sledz, C.A., et al., 2003. Activation of the interferon system by short-interfering RNAs. *Nat. Cell. Biol.* 5, 834–839.
- Sroka, H., et al., 1975. Ultrastructure of the syndrome of continuous muscle fibre activity. *Acta Neuropathol.* 31, 85–90.
- Toyka, K.V., et al., 1975. Myasthenia gravis: passive transfer from man to mouse. *Science* 190, 397–399.
- Tuschl, T., et al., 1999. Targeted mRNA degradation by double-stranded RNA in vitro. *Genes Dev.* 13, 3191–3197.
- VanSaun, M., et al., 2003. Structural alterations at the neuromuscular junctions of matrix metalloproteinase 3 null mutant mice. *J. Neurocytol.* 32, 1129–1142.
- Verschuuren, J.J., et al., 1990. Single-fiber electromyography in experimental autoimmune myasthenia gravis. *Muscle Nerve* 13, 485–492.
- Wood, S.J., Slater, C.R., 1995. Action potential generation in rat slow- and fast-twitch muscles. *J. Physiol.* 486 (Pt 2), 401–410.
- Wood, S.J., Slater, C.R., 1997. The contribution of postsynaptic folds to the safety factor for neuromuscular transmission in rat fast- and slow-twitch muscles. *J. Physiol.* 500 (Pt 1), 165–176.
- Wood, S.J., Slater, C.R., 2001. Safety factor at the neuromuscular junction. *Prog. Neurobiol.* 64, 393–429.
- Zhang, B., et al., 2007. Beta-catenin regulates acetylcholine receptor clustering in muscle cells through interaction with rapsyn. *J. Neurosci.* 27, 3968–3973.
- Zhang, B., et al., 2008. LRP4 serves as a coreceptor of agrin. *Neuron* 60, 285–297.